



Nonlinear 3D Finite Element Model for Square Composite Columns Under Various Parameters

Dara Anwer Mawlood¹, Dr. Serwan Khorsheed Rafiq², Muhammed Halkawt Abdullah³

¹ Water Resources Department, College of Engineering, University of Sulaimani, Kurdistan Region, Iraq, dara.mawloud@univsul.edu.iq

² Civil Engineering, College of Engineering, University of Sulaimani, Kurdistan Region, Iraq, serwan.rafiq@univsul.edu.iq

³ Civil Engineering, College of Engineering, University of Sulaimani, Kurdistan Region, Iraq, muhammed.abdullah@univsul.edu.iq

ARTICLE INFO

Article history:

Received 12/03/ 2022....

Received in revised form 28/05/ 2022.

Accepted 02/ 06/ 2022.

Available online 30 /07/ 2022

Keywords:

Eccentricity loading

CFSP (concrete filled steel pipe)

Finite element method

Nonlinear analysis

ABSTRACT

Composite columns are frequently used in constructing high-rise structures because they can minimize the size of the building's columns while increasing the floor plan's usable space. This study aims to create a nonlinear 3D finite element model for square composite columns designed for solid and hollow columns with various multi-skin tubes subjected to loads at eccentricities of (30 and 60) mm, compressive strength, and mesh size using the ABAQUS software. The comparison was based on the experimental data of six references of composite columns. While the compressive strength of concrete increases, the stiffness of the composite column rise. The ratio of concrete compressive strength values for composite column increased by (0, 12.3, 17.8, and 26.7 percent) for (f_c' =25, 31.96, 35, and 40) MPa, respectively. The results of the different mesh sizes (20, 40, and 60) mm are showing; The experimental results and the finite element solution developed using the (20 X20) mm element correspond well. The nonlinear finite element analysis method was used, and the finite element outputs results were confirmed to be in favorable agreement with the experimental data

DOI: [10.37650/ijce.2022.172882](https://doi.org/10.37650/ijce.2022.172882)

1. Introduction

Steel concrete composite constructions have been popular in recent years due to their increased load-carrying ability and rigidity, in comparison to steel or traditional concrete constructions. It could be employed in bridges, high-rise buildings, viaducts, and electrical transmission towers due to its significant structural performance (Perea, 2010, Papadrakakis & Fragiadakis, 2019). The advantages of both steel and concrete elements are optimally combined in the composite structure. The composite columns are extensively utilized in the development of high-rise structures because they can decrease the size of the building's columns while maximizing the floor plan's usable space. Furthermore, the composite column increases the overall rigidity of the structure and provides excellent shear resistance against large earthquakes and other lateral pressures (Karthek & Das, 2020). In ABAQUS 6.13-4, a 3D nonlinear analysis technique uses numerical solutions to simulate the finite element model and find defects in composite structural elements (Rafiq, 2017). This paper investigates the most effective nonlinear finite element model for analyzing solid and hollow composite columns with many layers of HSS (hollow steel structure) steel pipe under compression. Al-Khekany et al. Test results will be used to validate the

* Corresponding author. E-mail address: dara.mawloud@univsul.edu.iq

ABAQUS 6.13-4 software results (Al-Khekany et al., 2018). Then, based on correction factor that is obtained as a result of the finite element software and experimental data, we expanded data of a composite column under different eccentricity loads, different compressive strength of concrete and mesh size of the element by 3D nonlinear analysis ABAQUS 6.13-4 software. In the past, various researchers have studied on the behavior of composite structures, as Yonas T.Y. et al. (Yonas et al., 2018) used ABAQUS/static general analysis to model 18 different columns. The steel tube thickness, steel reinforcement ratio, column length, and depth to thickness ratio of 18 different reference columns were all varied. The results show that: A composite column with a smaller eccentricity, a big cross-sectional area and a large steel tube thickness may support a larger maximum load. The load carrying capacity reduces as eccentricity increases, while the mid-height displacement increases as the length increased. Peyman Beiranvand et al. (Anuntasena et al., 2019) provided a nonlinear 3-D finite element model for eccentrically loaded ten concrete encased steel composite columns. The model accounted for the interaction between the steel segment and the concrete. A variety of column dimensions, structural steel sizes, concrete strengths, and structural steel yield stresses have been considered. As eccentricity is reduced, the maximum allowable load is increased in concrete section.

Thunga Kartheek & T. Venkat Das (Kartheek & Das, 2020) In this study, the ABAQUS simulation of completely enclosed composite columns was compared to reinforced concrete columns of varying concrete strengths. For reinforced concrete and composite columns with I-section steel confinement, axial load capacity deformation, stress, and strain patterns are calculated. The finite element approach may be used by ABAQUS software to determine the behavior of composite and reinforced concrete columns. Reinforced concrete columns, according to the findings, are less resistant to ultimate axial stress than completely enclosed composite columns. Mohamed et al. (Ibrahim et al., 2017) This study presents the experimental test results and nonlinear finite element modeling of an experimental test program on concrete-filled steel tube CFST columns with longitudinal stiffeners as a recommended approach to increase CFST capacity. The validated numerical model is utilized to broaden the research to incorporate other parameters influencing CFST column design. The findings demonstrate that adding longitudinal stiffeners somewhat enhances load-carrying capacity, which may encourage the use of such a system to improve the load-carrying capacity of current CFST columns. Mohammed Salem and Muhammad Shekaib (Al-Ansari & Afzal, 2020) A mathematical approach for assessing uniaxial and biaxial reinforced concrete columns is proposed. This suggested model is a quick and easy way to analyze and build reinforced concrete columns that does not need interaction charts. The examined columns are also analyzed using computer software. The average gap between theoretically generated and finite element software values is less than 10%, indicating promising computational results.

The overall purpose of this research was to develop a nonlinear 3D finite element analysis model for square composite columns with changing applied load position, element Mesh size, buckling and compressive strength of concrete.

2. Modeling

This study used ABAQUS 6.13-4, and all simulations are produced using the standard/ Explicit model 3D nonlinear Analysis. As shown in Figures (1 and 2), the steel tube was modeled using a shell homogeneous Quad-dominated (Element Type for Meshing process), while the concrete infill was modeled using a solid homogeneous Hex (Element Type for Meshing process) as illustrated in Figures (3 and 4) (Abaqus, 2011). The supporting rigid plates at the top and bottom of the samples were modelled using a discrete rigid element. This study employed a concrete model with decreased plasticity to determine the plastic behavior of materials. The stress-strain curve can be determined using equations (1,2,3,4, and 5), the stress-strain curve may be used to calculate the mean compressive strength f_{cm} ; moreover, the stress-strain relationship for concrete and steel under uniaxial load of tension and compression can be depicted in Figure (5, and 6) (Kmieciak & Kamiński, 2011). Table (1, 2, and 3) shows the input data for the ABAQUS concrete damage plasticity model based on experimental results by Al-Khekany et al. (Al-Khekany et al., 2018).

$$E_{cm} = 22(0.1 f_{cm})^{0.3} \quad (1)$$

$$\epsilon_{c1} = 0.7(f_{cm})^{0.31} \quad (2)$$

$$\sigma = f_c (k\eta - \eta^2) / (1 + (k-2)\eta) \quad (3)$$

$$k=1.05E_{cm} \epsilon_{c1}/f_{cm} \tag{4}$$

$$\eta=\epsilon_c/\epsilon_{c1} \tag{5}$$

where:

f_{cm} is in MPa

E_{cm} is the longitudinal modulus of elasticity

ϵ_{c1} is strain at average compressive strength

ϵ_{cu} is the ultimate strain (3.5%)

Table 1: Concrete property, material data

Density (γ)	24000 N/m ³
Compressive strength of concrete (f'_c)	31.96E6 N/m ²
Young's modulus (E)	20000 N/m ²
Poisson's ratio (η)	0.2
Dilation Angle	30
Flow potential Eccentricity (ϵ)	0.1
* f_{b0}/f_{c0}	1.16
K	0.667
Viscosity parameter	0

* f_{b0}/f_{c0} is a ratio of the strength in the biaxial state to the strength in the uniaxial state.

* k can be defined as a function of void ratio.

Table 2: Steel tube property, material data

Density (γ)	78500 N/m ³
Young's modulus (E)	200000 N/m ²
Poisson's ratio (η)	0.3
Thickness (t)	4mm

Table 3: Plastic behavior of Steel tube property data

Tensile strength of steel (MPa)	Elongation (mm)
50	0
260	0.25

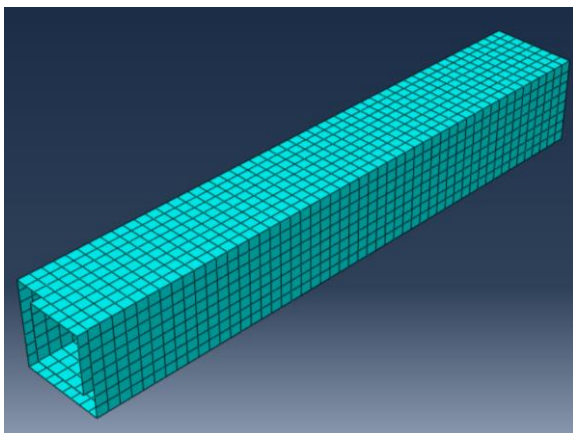


Fig. (1) Meshing of steel tube.

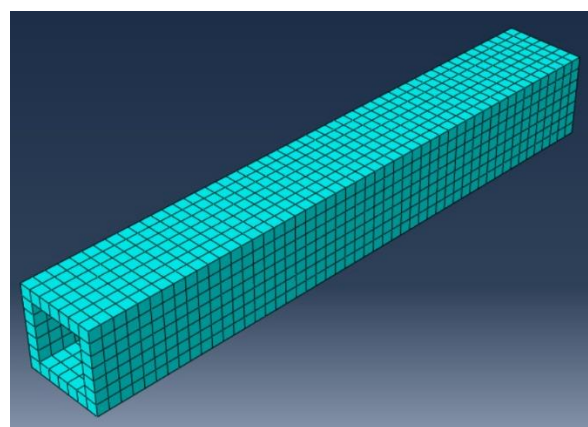


Fig. (2) Meshing for concrete.

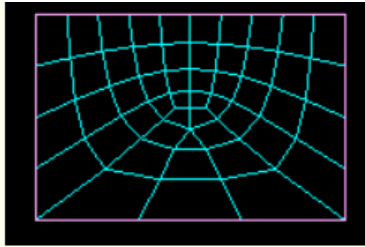


Fig. (3) Element type (Quad-dominated) for meshing steel tube.

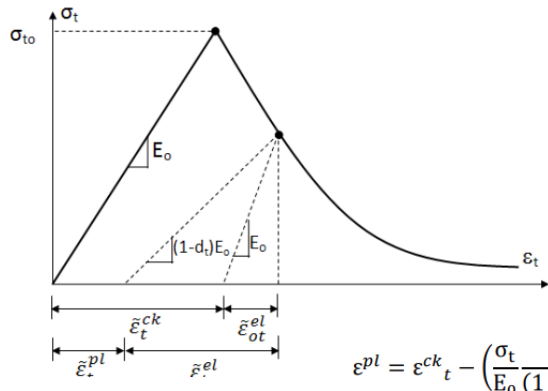
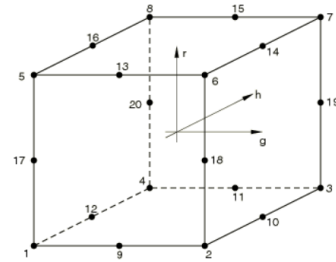
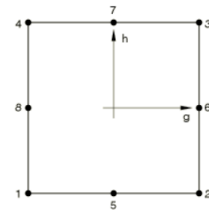


Fig. (4) Element type (Hex) for meshing concrete

$$\epsilon^{pl} = \epsilon^{ck}_t - \left(\frac{\sigma_t}{E_0} \frac{d_t}{1 + d_t} \right)$$

Fig. (5) Tension behaviour for steel in ABAQUS(Kmieciek & Kamiński, 2011)

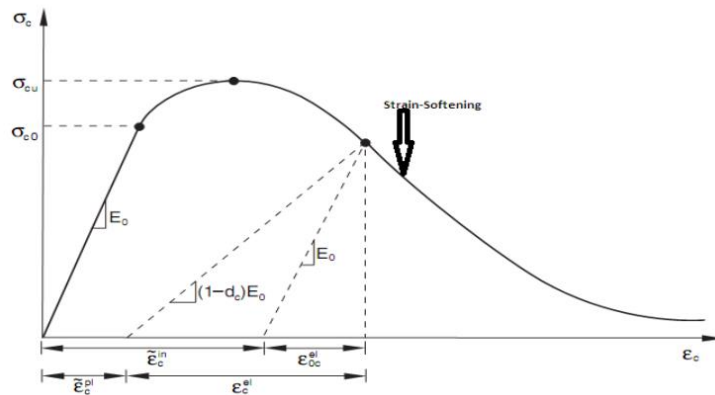


Fig. (6) Compression behavior for concrete in ABAQUS (Kmieciek & Kamiński, 2011)

3. Validation of The Model

Using data from Al-Khekany et al. (Al-Khekany et al., 2018), the structural behavior of solid and hollow composite columns reinforced with multi layers of HSS (Hollow Steel Structure) steel pipe under compression is studied. As part of the study, six specimens were tested. There are five composite samples and one non-composite sample. Figure (7) shows composite samples constructed normal strength concrete and HSS steel pieces with different amounts of HSS layers. All specimens have a column height of 1000mm, with a square column dimension of 150mm. (SN1H) was given to non-composite samples, while the composite samples were (SC2H, SC3H, SC1S, SC2S, SC3S). The first letter (S) represents the cross section of a square specimen, the second letter (C or N) indicates whether the part is composite or non-composite, HSS's layered number, given by numbers (1,2, and 3), henceforth the last letter (S or H) indicates whether the segment is Solid or Hollow. Figure (7) shows a drawing of the specimens.

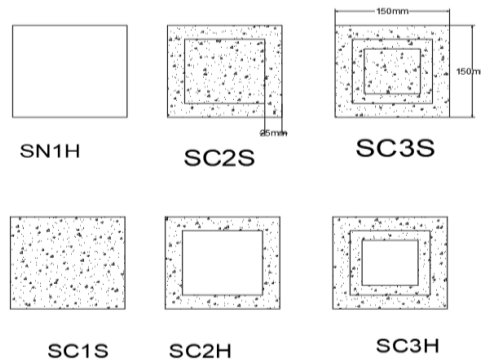


Fig. (7) Test of specimens

4. Finite Element Modeling

Experimenting with a composite column specimen is both time consuming and expensive. Using finite element analysis and considering the impact of various parameters on the behavior of such columns may offer an alternative solution to save time and cost. ABAQUS is used to generate a numerical model of composite columns using finite element code. Geometric and material non-linearity were included in the finite element model.

The cross-section of the composite column was set at 150mm square. Based on the six references of composite columns that Al-Khekany's et al. evaluated in the laboratory under concentrically loaded conditions. Therefore, comparing experimental data with numerical results generated by the ABAQUS 6.13-4 program with variable eccentricity loads (30 and 60) mm, resulted in different compressive strength of concrete, and affected the meshing size of the composite columns.

4.1 Effect of Mesh size on the Models

The experimental results were compared to the numerical results of analysis based on these meshes. A shell homogeneous Quad-dominated (Element Type for Meshing process) was used to model the steel tube, whereas a solid homogeneous Hex (Element Type for Meshing process) was used to model the concrete infill. A discrete rigid element was used to model the supporting rigid plates at the top and bottom of the samples. For the specimens (SC2H, SC2S, and SC2H) Different mesh components were chosen to explore the effect of finer or coarser mesh on the analyses' outcomes (20, 40, and 60) mm of the mesh sizes. Finally, the best results were chosen, which were close to the experimental results. The finite element solution produced using the (20 X 20) mm element is in adequate agreement with the experimental curve, as shown in Figure (8).

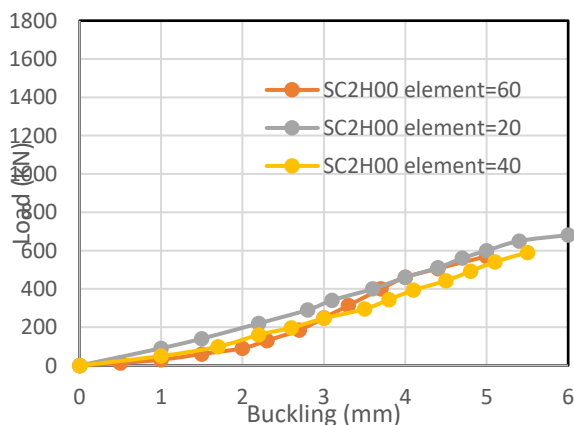


Fig. (8-a) Load-buckling curve for different mesh size for specimen (SC2H00)

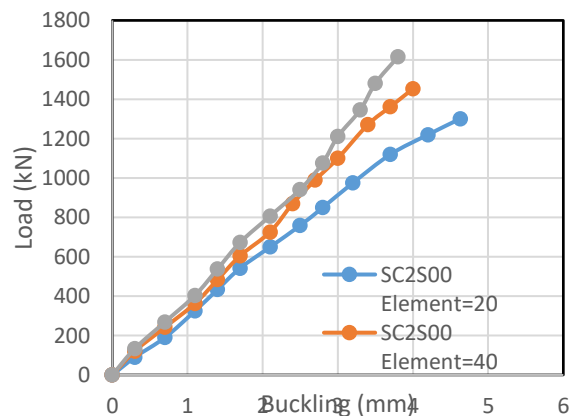


Fig. (8-b) Load-buckling curve for different mesh size for specimen (SC2S00)

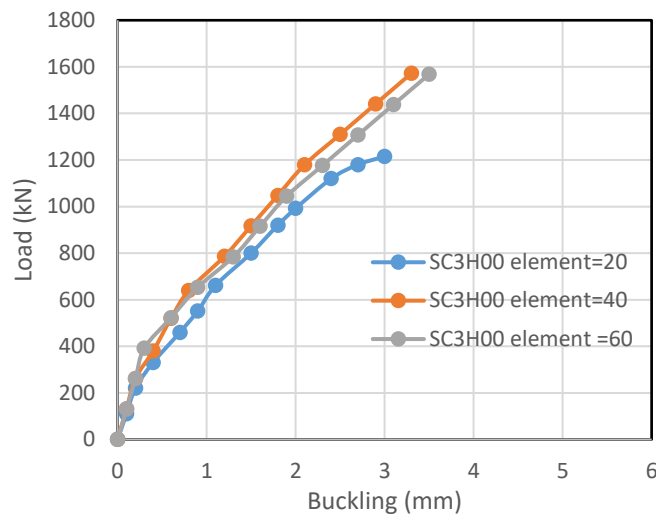


Fig. (8-c) Load-buckling curve for different mesh size for specimen (SC3H00)

5. Finite Element Results and Discussion

The failure patterns for composite columns that were tested under load using the numerical data derived from the ABAQUS 6.13-4 program show that; all the specimens failed due to local buckling failure similar to Al-Khekany's et al. laboratory's study, as illustrated in Figure (9). The specimens (SC2S00, SC3H00, and SC2H00) are analyzed using ABAQUS program then compared with experimental data the difference of ratio were (4.8, 8.5, and 12.8) percent respectively, as shown in Figure (10,11, and 12), and illustrated in Table (4). As the section's strength and ductility are enhanced by filling the tube with concrete, the steel tube's local buckling failure is delayed. The steel tube confines the concrete, which prevents local buckling failure of hollow steel tubes due to the restraining influence of concrete. The specimens (SC2S, SC2H, and SC3H) were analysis by ABAQUS 6.13-4 for different parameters, as illustrated below:

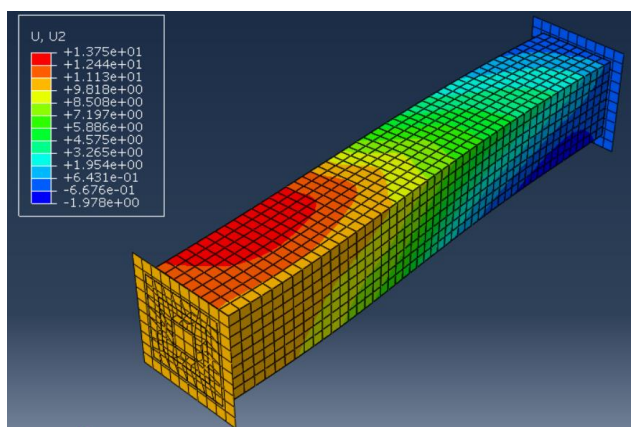


Fig. (9-a) Column failure under eccentricity (SC3H)

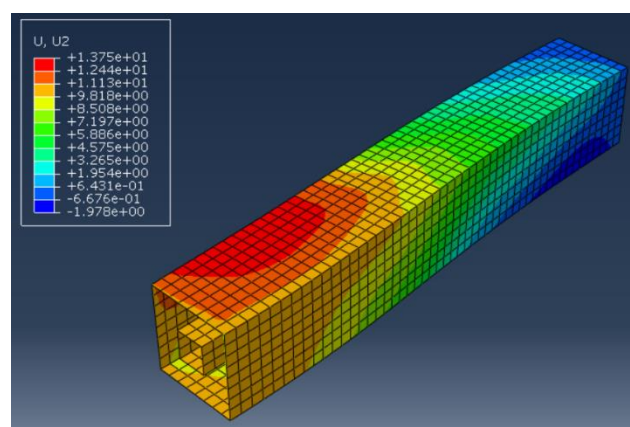


Fig. (9-b) Steel tube failure under eccentricity (SC3H)

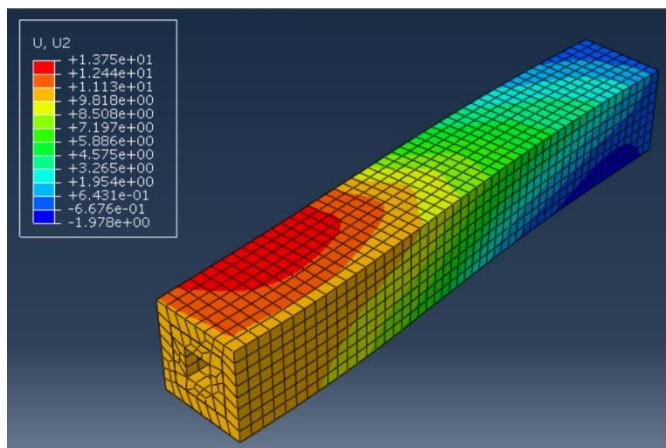


Fig. (9-c) Concrete failure under eccentricity (SC3H)

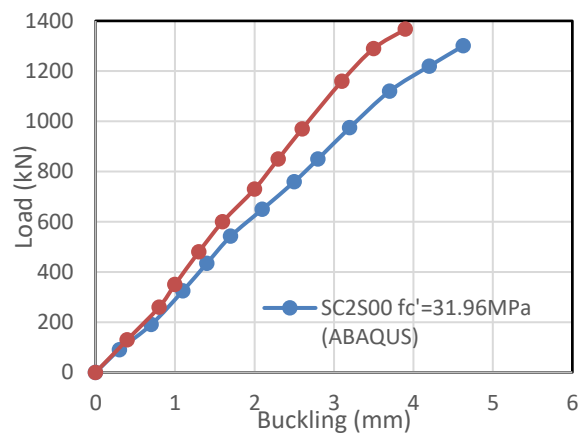


Fig. (10) Load-buckling curve (SC2S00)

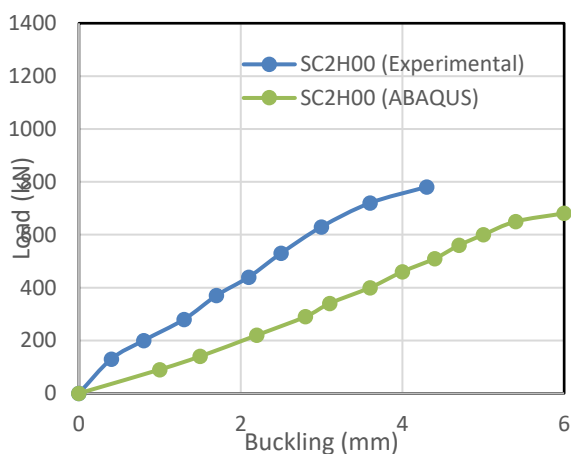


Fig. (11) Load-buckling curve (SC3H00)

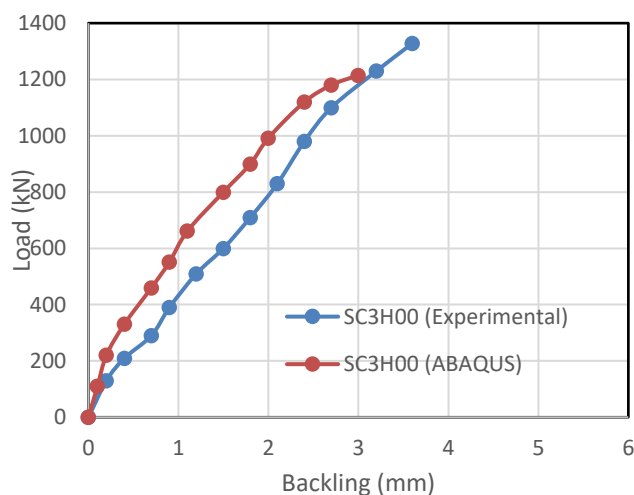


Fig. (12) Load-buckling curve (SC2H00)

Table 4: Experimental vs ABAQUS results

Specimens	Ultimate loads (kN) Experimental	Ultimate loads (kN) ABAQUS	Difference (%)= (Exp.- ABAQUS.)/Exp.
SC2H00	781	681	12.8
SC2S00	1367	1301	4.8
SC3H00	1328	1215	8.5

*00 refers to eccentricity of loads is zero.

5.1 Eccentricity Effect

Table (5) shows that when the eccentricity of applied loads increases, the amount of loads to failure decreases for composite columns (SC3H) under various eccentricities (0, 30, and 60) mm. The results reveal that the difference ratio of ultimate loads varies between (0, 35 and 39) percent for square composite columns, respectively. As shown in Figure (13).

Table-5 Effect of different eccentricity for (SC3H)

Eccentricity (mm)	ABAQUS Load (kN)	Difference%=(e0-ei)/e0
0	1215	0
30	785	35
60	740	39

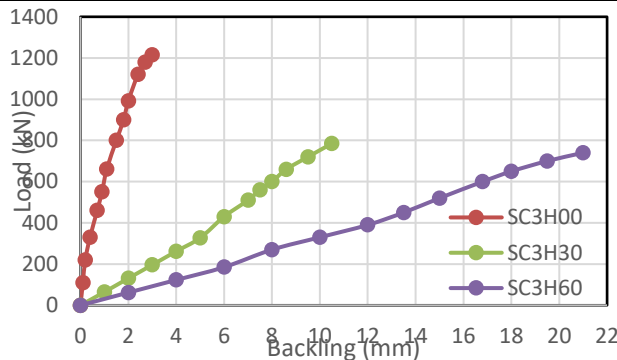


Fig. (13-a) Load-buckling curve (SC3H) for different eccentricity

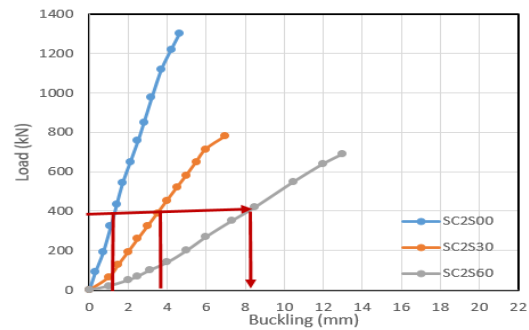


Fig. (13-b) Load-buckling curve (SC2S) for different eccentricity

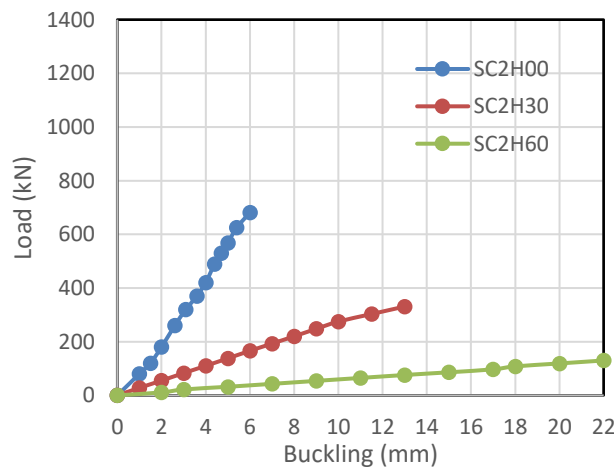


Fig. (13-c) Load-buckling curve (SC2H) for different eccentricity

5.2 Compressive Strength Effect

In this part, the specimen (SC2S) was simulated under vertical loading; the key difference is the concrete strength (25MPa, 31.96MPa, 35MPa, and 40MPa) as shown in Table (6), compared to the compressive strength (25MPa) as reference, the ratio of differences with reference were (0, 12.3, 17.8 and 26.7) percent, respectively. The results of ABAQUS shows that concrete strength have a substantial impact on stiffness. It has been proven that when concrete strength improves, the column stiffness increases. As illustrated in Figure (14).

Table-6 Effect of compressive strength of concrete for specimens (SC2S00)

Concrete compressive strength ($f'c$)	ABAQUS Load (kN)	Difference%=(Load(i)-Load(25))/Load(25)
25	1154	0
31.96	1301	12.3
35	1360	17.8
45	1462	26.7

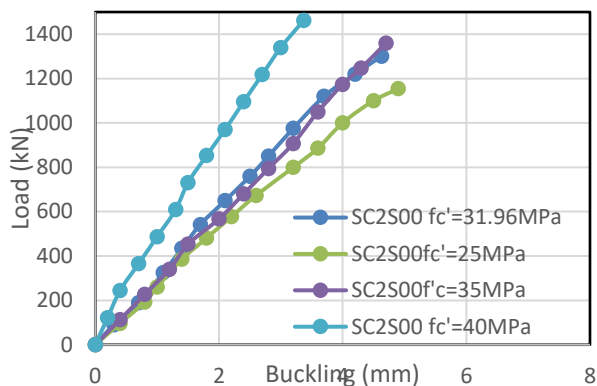


Fig. (14-a) Load-buckling curve (SC2S00) for different compressive strength

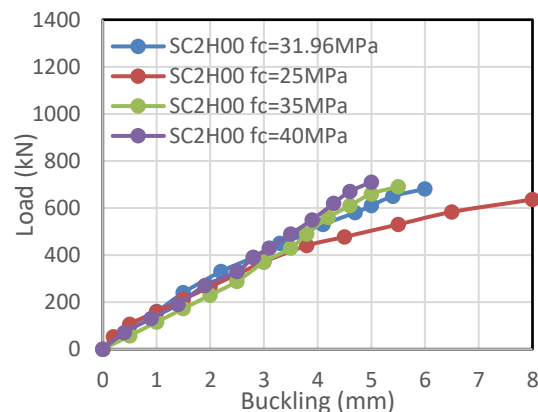


Fig. (14-b) Load-buckling curve (SC2H00) for different compressive strength

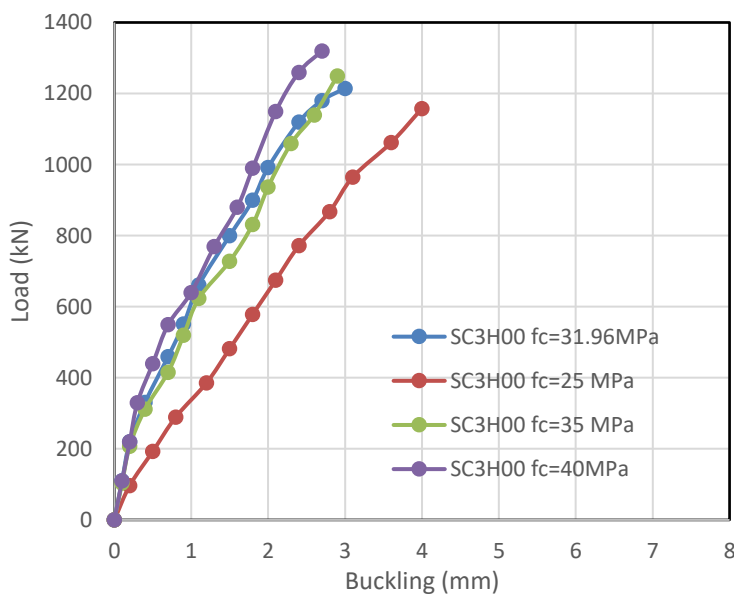


Fig. (14-c) Load-buckling curve (SC3H00) for different compressive strength

5.3 Buckling Effect

The findings show that load eccentricity has a considerable impact on the critical force associated with local column buckling. The existence of load eccentricity applied in a direction away from the column's web has been observed to result in a considerable reduction in the critical load. Figure (13-b) illustrates the specimen SC2S by ABAQUS numerical data. From Table (7), when the load is fixed at 400 kN the buckling ratio increased by (0, 200, and 531) percent for specimens (SC2S00, SC2S30, and SC2S60) respectively under the effect of eccentricities.

Table-7 Effect of different eccentricity for (SC2S)

Eccentricity (mm)	ABAQUS Buckling (mm)	Difference%=(ei-e0)/e0
0	1.3	0
30	3.9	200
60	8.2	531

6. Conclusion

- The proposed finite element models utilized in this study are capable of predicting composite column specimen behavior. The numerical results were in good agreement with the experimental load-buckling curve throughout the whole range of behavior.
- The suggested model findings reveal that as the eccentricity of applied loads increases from 30mm to 60mm, the quantity of loads on composed columns decreases by (0, 35 and 39) percent, respectively.
- The strength of concrete has a significant impact on specimen (SC2S00) stiffness. The stiffness of the composite column increases as the concrete strength increases. For (25, 31.96, 35, and 40) MPa, the ratio of concrete compressive strength values for composite column increased by (0, 12.3, 17.8, and 26.7%), respectively.
- the finite element solution generated using the (20 X20) mm element agrees with the experimental data, the differences mesh size (20, 40, and 60) mm, show that element size 20mm more approach in chart.
- The model findings show that; the load eccentricity has a considerable impact on the critical force associated with column buckling. The existence of load eccentricity applied in a direction away from the web (side) of the column has been observed to result in a significant reduction in the critical load.

References

- Abaqus, G. (2011). Abaqus 6.11. *Dassault Systemes Simulia Corporation, Providence, RI, USA*.
- Al-Ansari, M. S., & Afzal, M. S. (2020). Mathematical Model for Analysis of Uniaxial and Biaxial Reinforced Concrete Columns. *Advances in Civil Engineering*, 2020.
- Al-Khekany, A. M., Al-Yassri, L. S., & Abbas, H. S. (2018). An experimental investigation of hollow composite column reinforced by multi-skin square and round steel tube. *International Journal of Civil Engineering and Technology*, 9(11), 784–793.
- Anuntasena, W., Lenwari, A., & Thepchatri, T. (2019). Finite element modelling of concrete-encased steel columns subjected to eccentric loadings. *Engineering Journal*, 23(6), 299–310.
- Ibrahim, M., Elabd, M., & Kandeel, K. (2017). Experimental and Numerical Behaviour of CFST Columns with Longitudinal Stiffeners. *ERJ. Engineering Research Journal*, 40(3), 197–209.
- Kartheek, T., & Das, T. V. (2020). 3D modelling and analysis of encased steel-concrete composite column using ABAQUS. *Materials Today: Proceedings*, 27, 1545–1554.
- Kmieciak, P., & Kamiński, M. (2011). Modelling of reinforced concrete structures and composite structures with concrete strength degradation taken into consideration. *Archives of Civil and Mechanical Engineering*, 11(3), 623–636.
- Papadrakakis, M., & Fragiadakis, M. (2019). *Analysis of rectangular concrete-filled double skin tubular short columns with external stainless steel tubes omnia kharoob1, Nashwa Yossef2*.
- Perea, T. (2010). *Analytical and experimental study on slender concrete-filled steel tube columns and beam-columns*. Georgia Institute of Technology.
- Rafiq, S. K. (2017). Non Linear Finite Element Modeling of Reinforced Concrete Flat Plate Slabs with openings. *Sulaimania Journal for Engineering Sciences*, 4(4).
- Yonas, T., Temesgen, W., & Senshaw, F. (2018). Finite element analysis of slender composite column subjected to eccentric loading. *International Journal of Applied Engineering Research*, 13(15), 11730–11737.